DEPARTMENT OF THE ARMY
US ARMY RESEARCH, DEVELOPMENT AND ENGINEERING COMMAND
ARMY RESEARCH LABORATORY
ABERDEEN PROVING GROUND MD 21005-5068

REPLY TO ATTENTION OF

AMSRD-ARL-WM-BC 6 March 2006

MEMORANDUM FOR SEE DISTRIBUTION

SUBJECT: ARL-TR-3653, "Base Pressure Computations of the Defence Evaluation and Research Agency Generic Missile Wind Tunnel Model," by James DeSpirito

Errata sheet attached (encl) for the above-listed report.

Encl

James DeSpirito
Aerodynamics Branch

ERRATA SHEET

re: ARL-TR-3653, “Base Pressure Computations of the Defence Evaluation and Research Agency Generic Missile Wind Tunnel Model,” by James DeSpirito, September 2005

Replace previous version of this report that was distributed on 2/28/06 with new report attached.

Reason: During the final printing of all copies of this report, the ink either ran out or bled, causing poor quality color on figures 2 through 9.

AMSRD-ARL-WM-BC
DISTRIBUTION:

1 (PDF ONLY) DEFENSE TECHNICAL INFORMATION CTR
DTIC OCA
8725 JOHN J KINGMAN RD
STE 0944
FORT BELVOIR VA 22060-6218

1 US ARMY RSRCH DEV & ENGRG CMD
SYSTEMS OF SYSTEMS INTEGRATION
AMSRD SS T
6000 6TH ST STE 100
FORT BELVOIR VA 22060-5608

1 INST FOR ADVNCD TCHNLGY
THE UNIV OF TEXAS
AT AUSTIN
3925 W BRAKER LN
AUSTIN TX 78759-5316

1 DIRECTOR
US ARMY RESEARCH LAB
IMNE ALC IMS
2800 POWDER MILL RD
ADELPHI MD 20783-1197

3 DIRECTOR
US ARMY RESEARCH LAB
AMSRD ARL CI OK TL
2800 POWDER MILL RD
ADELPHI MD 20783-1197

3 DIRECTOR
US ARMY RESEARCH LAB
AMSRD ARL CS IS T
2800 POWDER MILL RD
ADELPHI MD 20783-1197

ABERDEEN PROVING GROUND

1 DIR USARL
AMSRD ARL CI OK TP (BLDG 4600)

AMSRD-ARL-WM-BC
DISTRIBUTION:

1 AFRL/MNAV
G ABATE
101 W EGLIN BLVD STE 332
EGLIN AIR FORCE BASE FL 32542

1 AEROPREDICTION INC
F MOORE
9449 GROVER DR STE 201
KING GEORGE VA 22485

1 UNIV OF TEXAS AT ARLINGTON
MECHANICAL AND AEROSPACE
ENGR DEPT
J C DUTTON
BOX 19018
500 W FIRST ST
ARLINGTON TX 76019-0018

3 COMMANDER USAAMCOM
AMSAM RD SS AT
R KRETZSCHMAR
L AUMAN
E VAUGHN
REDSTONE ARSENAL AL 35898-5252

ABERDEEN PROVING GROUND

16 DIR USARL
AMSRD ARL CI HC
R NOAK
AMSRD ARL WM
J SMITH
AMSRD ARL WM B
T ROSENBERGER
AMSRD ARL WM BA
J DESPIRITO (3 CPS)
B GUIDOS
K HEAVEY
P PLOSTINS
J SAHU
S SILTON
P WEINACHT
AMSRD ARL WM BD
B FORCH
M LEADORE
AMSRD ARL WM BF
H EDGE
S WILKERSON

AMSRD-ARL-WM-BC
DISTRIBUTION:

1 DSTL BEDFORD
T BIRCH
BLDG 115 RM 125
BEDFORD TECHNOLOGY PARK
BEDFORD
MK44 2FQ
UK

1 DSTL FORT HALSTEAD
J EDWARDS
SEVENOAKS KENT
TN 14 7BP
UK

2 DEFENCE RSCH AND
DEV CANADA-VALCARTIER
F LESAGE
E FOURNIER
2459 PIE XI BLVD N
VAL-BELAIR (QC) G3J1X5
CANADA

1 DEFENCE SCIENCE AND
TECHNOLOGY ORGANIZATION
V BASKARAN
BLDG 11 RM 119
506 LORIMER ST
FISHERMANS BEND
VICTORIA 3207
AUSTRALIA

ARMY RESEARCH LABORATORY

Base Pressure Computations of the DERA Generic Missile Wind Tunnel Model

by James DeSpirito

ARL-TR-3653 September 2005

NOTICES

Disclaimers

The findings in this report are not to be construed as an official Department of the Army position unless so designated by other authorized documents.

Citation of manufacturer's or trade names does not constitute an official endorsement or approval of the use thereof.

Destroy this report when it is no longer needed. Do not return it to the originator.

Army Research Laboratory
Aberdeen Proving Ground, MD 21005-5066

ARL-TR-3653 **September 2005**

Base Pressure Computations of the DERA Generic Missile Wind Tunnel Model

James DeSpirito
Weapons and Materials Research Directorate, ARL

REPORT DOCUMENTATION PAGE

Form Approved
OMB No. 0704-0188

1. REPORT DATE *(DD-MM-YYYY)*	2. REPORT TYPE	3. DATES COVERED (From - To)
September 2005	Final	November 1999–May 2000

4. TITLE AND SUBTITLE
Base Pressure Computations of the DERA Generic Missile Wind Tunnel Model

5a. CONTRACT NUMBER

5b. GRANT NUMBER

5c. PROGRAM ELEMENT NUMBER

6. AUTHOR(S)
James DeSpirito

5d. PROJECT NUMBER
1L1626I8AH80

5e. TASK NUMBER

5f. WORK UNIT NUMBER

7. PERFORMING ORGANIZATION NAME(S) AND ADDRESS(ES)
U.S. Army Research Laboratory
ATTN: AMSRD-ARL-WM-BC
Aberdeen Proving Ground, MD 21005-5066

8. PERFORMING ORGANIZATION REPORT NUMBER
ARL-TR-3653

9. SPONSORING/MONITORING AGENCY NAME(S) AND ADDRESS(ES)

10. SPONSOR/MONITOR'S ACRONYM(S)

11. SPONSOR/MONITOR'S REPORT NUMBER(S)

12. DISTRIBUTION/AVAILABILITY STATEMENT
Approved for public release; distribution is unlimited.

13. SUPPLEMENTARY NOTES

14. ABSTRACT

Computational fluid dynamic simulations were used to compute the aerodynamic coefficients of a body-alone missile and a planar fin missile in the presence of a wind tunnel sting. The investigation was an extension to a previous investigation in which the computed forebody axial force did not compare well with experimental wind tunnel data, while all other forces and moments showed excellent agreement. The current investigation showed that the computed results are accurate, predicting the total axial force to within 5% of the experimental values. The results indicate that the discrepancy in the forebody axial force is due to an inaccurate experimental base pressure measurement.

15. SUBJECT TERMS
aerodynamics, computational fluid dynamics, Magnus

16. SECURITY CLASSIFICATION OF:			17. LIMITATION OF ABSTRACT	18. NUMBER OF PAGES	19a. NAME OF RESPONSIBLE PERSON
a. REPORT	b. ABSTRACT	c. THIS PAGE			James DeSpirito
UNCLASSIFIED	UNCLASSIFIED	UNCLASSIFIED	UL	24	19b. TELEPHONE NUMBER (*Include area code*) (410) 278-6104

Contents

List of Figures

List of Tables

Acknowledgments

The author would like to thank Graham Simpson and Anthony Sadler (currently retired) of the former Defence Evaluation and Research Agency, United Kingdom, for providing the comprehensive database of wind tunnel test data and additional information. Thanks are also due to support engineers at Fluent, Inc. This work was supported in part by a grant of high performance computing time from the Department of Defense High Performance Computing Center at Aberdeen Proving Ground, MD.

INTENTIONALLY LEFT BLANK.

1. Introduction

The U.S. Army Research Laboratory completed a computational fluid dynamics (CFD) study of the aerodynamics of a generic missile in several configurations in 2000 (*1*, *2*). The primary purpose of the study was to investigate the aerodynamics of a missile with grid fin tail controls, but the body-alone configuration and conventional planar fins were also investigated. In general, the CFD computations showed excellent agreement with the experimental wind tunnel data. However, as described in DeSpirito et al. (*1*, *2*), the difference between the experimental and computed forebody axial force was about 17% in the planar fin case, much higher than in the body-alone (4%) and grid fin (3%–6%) cases.

The computations in DeSpirito et al. (*1*, *2*) did not model the missile wake flow. Therefore, total axial force, as measured by the wind tunnel balance, could not be directly compared. Instead, the forebody axial force, which has the force due to the pressure on the base of the missile removed, was compared. The determination of the experimental forebody axial force relies on the accurate measurement of the pressure on the base of the wind tunnel model.

It was decided to further use CFD to investigate the pressure distribution near the base of the wind tunnel model in the presence of the sting. A possibility to be explored was whether there was a large nonuniformity of the pressure on the base of the wind tunnel model in the planar fin case, as compared to the body alone case. With a highly nonuniform pressure on the base it is possible that an incorrect base pressure correction would be applied in determining the forebody axial force in the experimental data. In general, the Defence Evaluation and Research Agency (DERA) wind tunnel data was of excellent quality. However, the results of this investigation did indicate that the base pressure correction in the wind tunnel results were inaccurate in the planar fin configuration (*3*). This report provides an expanded discussion of the results than was possible in DeSpirito et al. (*3*).

2. Numerical Approach

The wind tunnel results and the dimensions of the geometric models were supplied by the former DERA. In 2001, DERA was separated into two organizations: QinetiQ, an independent science and technology company, and the Defence Science and Technology Laboratory, an agency of the United Kingdom Ministry of Defence. The generic missile consisted of a 3-cal tangent ogive, followed by a 10-cal body (1 cal = 94 mm). Figure 1 shows the CFD models including the section of the sting that was modeled. The four fins were located 1.5 cal forward of the base. The configurations were labeled according to the designations used at DERA: the B1A

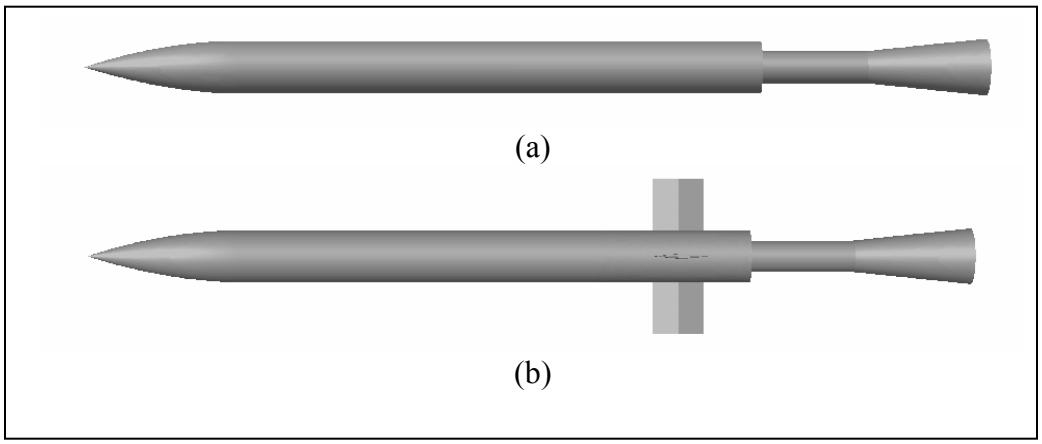

Figure 1. CFD model geometry for (a) B1A and (b) B1AC2R.

configuration was the body-alone case and the B1AC2R was the planar fin case. The grid fin case (B1AL2R) was not investigated with the wind tunnel sting modeled. The span and chord of the planar fin were each 1.0 cal. The diameter of the cylindrical portion of the sting was 0.61 cal and was 2.0 cal long. The conical section had a rear diameter of 1.1 cal and a length of 2.3 cal. All analyses were performed at Mach 2.5 and at three angles of attack: $\alpha = 0°$, 10°, and 20°. The simulations were performed with the missile in the cruciform (+) configuration, and symmetry (*x*-*z* plane) was used so that only a half-plane was modeled.

The geometry and unstructured meshes for the three configurations were generated using the preprocessor, GAMBIT, supplied in the FLUENT software suite. Figures 2 and 3 show some characteristics of the meshes used for the B1A and B1AC2R configurations. In generating the meshes, boundary layer mesh spacing was used near the missile body and fin surfaces. Advantage was taken of the wall function option of the solver in FLUENT, and the first edge away from the wall surface was about 0.004 cal. (Since the cell center is the critical location in the solver, the distance used for y+ calculation is then 0.002 cal.) All mesh stretching was kept below a ratio of 1.2. Hexahedral cells were used except for a small region ahead of, and partly over, the first 0.1 cal of the nose of the missile (1% of the total length). This latter region was made up of tetrahedrons and pyramid transition elements. The tetrahedral mesh was made to cover a small part of the missile nose to allow a transition from the missile nose to the free-stream part of the mesh ahead of the missile. This approach was used because of a limitation in the early version of GAMBIT, which was removed in a later release of the software. Therefore, a true boundary layer-type mesh was not covering the first 1% of the missile body, but this had no observable effect on the results. The total number of cells in the B1A case was about 1.4 M, with only 4.4% consisting of nonhexahedral cells. The total number of cells in the B1AC2R case was about 1.9 M cells, with only 4.2% consisting of nonhexahedral cells.

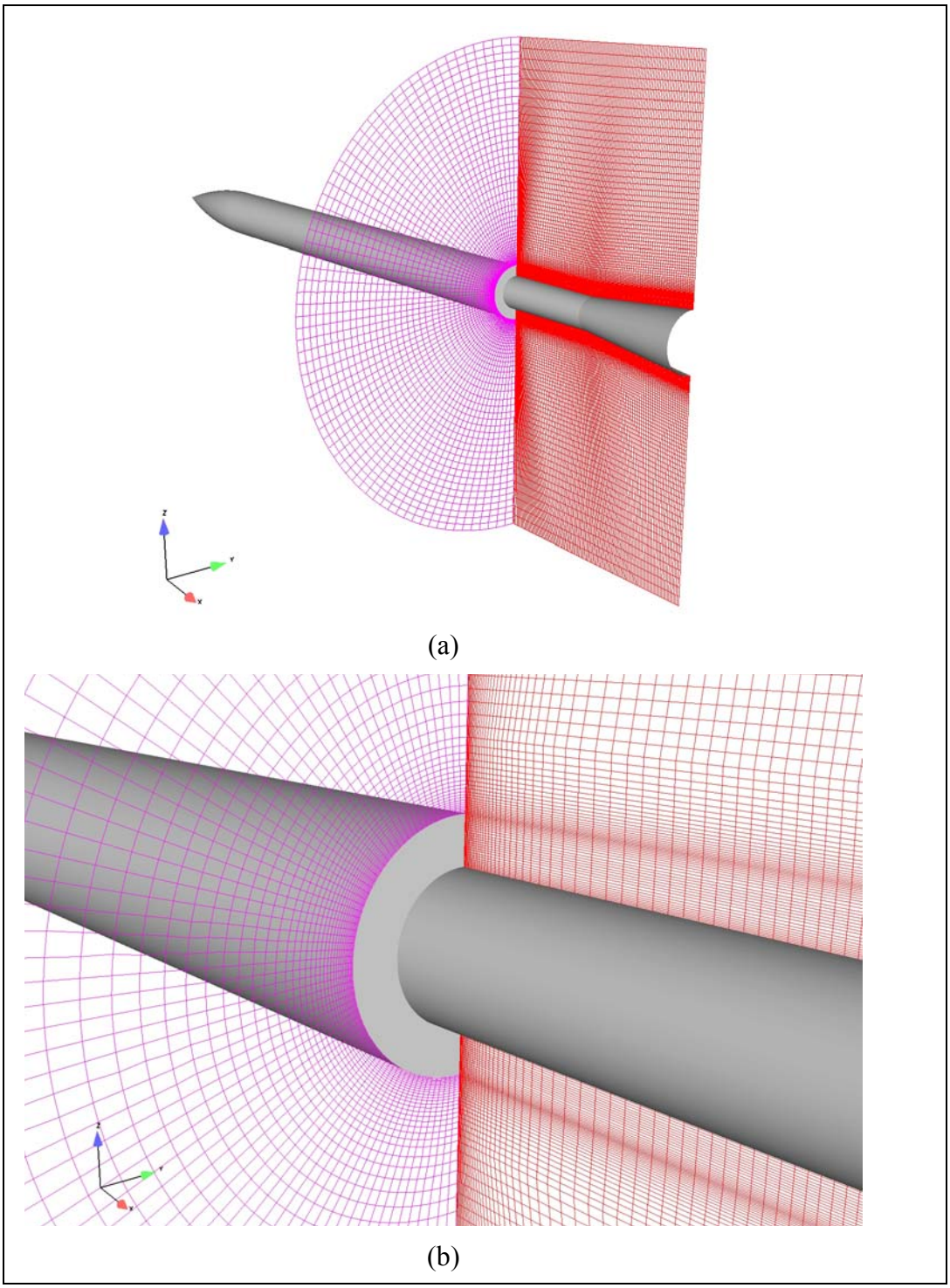

Figure 2. Computational mesh in sting region of B1A configuration.

The base flow was not simulated in the original calculations without the sting, so the mesh stopped at the end of the missile. For the current calculations, the geometry and mesh were extended to include a section of the sting, as shown. The computational domain extended 4 cal from the missile body. About 72 cells were used on the missile body in the circumferential

direction, with this value increased in the fin region (figure 3). The density of the mesh in the sting region was sufficient to resolve the features of the wake flow, albeit a steady-state idealization of such flow. It must also be noted that the annular base of the missile is a simplification of the actual experimental model, as determined from drawings. The sting actually protrudes into the hollow missile model for about 860 mm. The radial gap between the sting and the model is about 10 mm for the first 60 mm from the missile base, then 3 mm for the remaining distance inside the cavity.

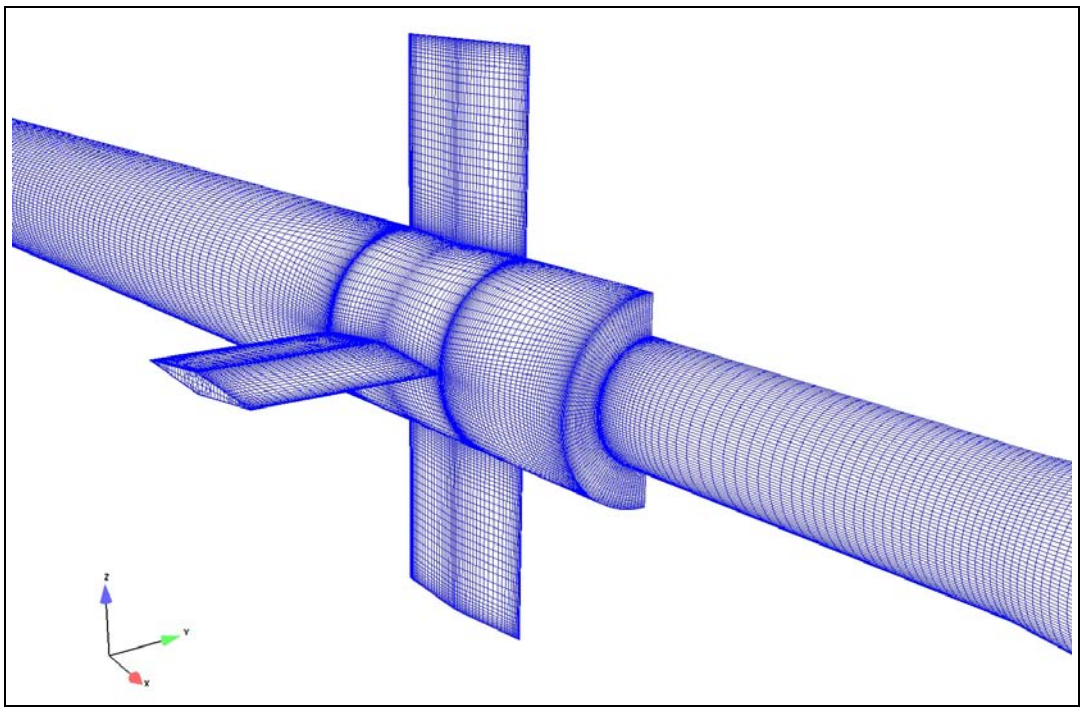

Figure 3. Computational mesh on surface of B1AC2R configuration.

Free-stream conditions for Mach 2.5 were set on the fluid boundaries. A no slip wall boundary condition was used for all solid surfaces. The y^+ value was about 40–60 along the missile body and about 150 along the ogive. The Reynolds number was 13.1×10^6 m^{-1} and the free-stream temperature and pressure were 137 K and 8325 Pa, respectively.

The commercial CFD code, FLUENT Version 5.1, was used to compute the steady-state solution of the flow field. The implicit, coupled, unstructured solver was used. The three-dimensional, time-dependent, Reynolds-Averaged Navier-Stokes equations are solved using the finite volume method. In the implicit solver, each equation in the coupled set of governing equations is linearized implicitly with respect to all dependent variables in the set, resulting in a block system of equations. A block Gauss-Seidel, point implicit linear equation solver is used with an algebraic multigrid method to solve the resultant block system of equations. The coupled set of governing equations is discretized in time and time marching proceeds until a steady-state

solution is reached. In the implicit scheme, which was used in this study, an Euler implicit discretization in time is combined with a Newton-type linearization of the fluxes.

The Spalart-Allmaras (*4*), one-equation turbulence model was used for these calculations. In FLUENT, the original version of the Spalart-Allmaras model is modified to allow the use of wall functions when the mesh resolution is not sufficiently fine to resolve the viscous-affected, near-wall region of the boundary layer (*5*). Second-order discretization was used for the flow variables and the turbulent viscosity equation.

The simulations were performed in parallel using 4–6 processors on a Silicon Graphics Onyx 2 with R12000 processors. The number of processors was limited by the software license in place at the time. The solutions were started with a Courant-Friedrich-Lewy (CFL) number of either 1.0 or 2.0. The CFL number was quickly increased to 4.0 or 5.0 for the remainder of the run. Convergence was determined by tracking the change in the aerodynamic coefficient values and the flow residuals during the solution. The aerodynamic coefficients converged in about 600 iterations. It took about 1500 iterations for the turbulent viscosity to converge, with the scaled residual reduced to about 10^{-6}.

3. Results and Discussion

The results for the configurations without the sting are summarized in table 1. The normal force and pitching moment coefficients are also shown in the table. The pitching moment and normal force were computed to within 4% and 2%, respectively. The difference between the calculated and experimental forebody axial force coefficient, C_x, was between 0.5% and 4.2% for the body-alone (B1A) case. However, for the planar fin (B1AC2R) case, the difference ranged from 16.2% to 17.4%. These results are also shown graphically in figure 4, which clearly shows the computed planar fin forebody axial force much lower than the experimental values.

Table 2 summarizes the results of the computations with the wind tunnel sting included. The computed pitching moment and normal force again compared very well with the experimental data–to within 2% and 1%, respectively. Also included in this table are listings of the total axial force, $(C_x)_{Bal}$, which is actually measured by the wind tunnel force balance, and the missile base pressure, C_{pb}, which were not available in the earlier CFD calculations performed without a wake flow. The base pressure, which is the negative of the axial base drag, $C_{pb} = -C_{xb}$, is used with $(C_x)_{Bal}$ to determine the forebody axial force, C_x (i.e., $(C_x)_{Bal} + C_{pb} = C_x$). The measured pressure on the base of the model must therefore be an accurate representation of the average base pressure in order to get an accurate forebody axial force from the experimental data.

Table 1. Aerodynamic coefficients for B1AC2R and B1A cases (no sting).

Case	α (°)	C_m			C_z			C_x		
		Fluent	**Exp.**	**%**	**Fluent**	**Exp.**	**%**	**Fluent**	**Exp.**	**%**
BIA	0	0.000	–0.031	—	0.000	0.005	—	0.1837	0.1895	–3.1
	10	–4.45	–4.448	+0.1	0.961	0.981	–2.0	0.1919	0.1928	–0.5
	14	–10.49	–10.13	–3.6	1.919	1.897	+1.2	0.1977	0.1936	+2.1
	20	–21.36	–21.07	–1.4	3.548	3.543	+0.1	0.2098	0.2014	+4.2
B1AC2R	0	–0.004	0.041	—		–0.002	—	0.2922	0.3513	–16.8
	10	–17.27	–16.97	–1.8	2.060	2.065	–0.2	0.3095	0.3746	–17.4
	20	–43.61	–43.31	–0.7	5.454	5.465	–0.2	0.3349	0.3996	–16.2

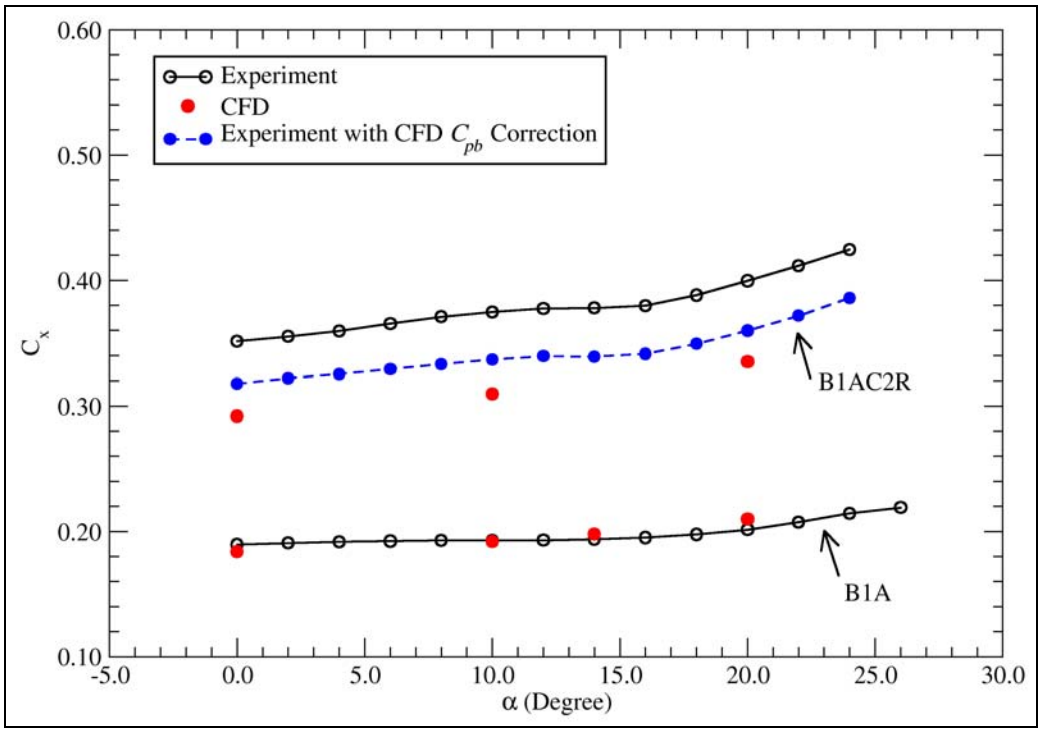

Figure 4. Forebody axial force coefficient vs. α for B1A and B1AC2R cases.

For the B1A configuration, it is seen from table 2 that the agreement of both the forebody axial force and the total axial force is very good–generally less than 5%. In the B1AC2R configuration, the computed total axial force compares very well with the experimental values–again less than 5%. The comparison of total axial force is shown graphically in figure 5, which shows that the CFD computations are predicting the flow field very well.

Table 2. Aerodynamic coefficients for B1AC2R and B1A cases.

Case/α		C_m	C_z	C_x	$(C_x)_{Bal}$	C_{pb}
B1A						
0°	Exp.	–0.031	0.005	0.1895	0.3149	–0.1254
	Fluent	0.000	0.000	0.1836	0.3241	–0.1405
	(% diff.)	—	—	(–3.1)	(+2.9)	(–12.0)
10°	Exp.	–4.448	0.981	0.1928	0.3429	–0.1501
	Fluent	–4.440	0.960	0.1919	0.3591	–0.1672
	(% diff.)	(–0.2)	(–0.2)	(–4.7)	(+4.7)	(–11.4)
20°	Exp.	–21.07	3.543	0.2014	0.3727	–0.1713
	Fluent	–21.20	3.523	0.2123	0.3964	–0.1841
	(% diff.)	(+0.6)	(–0.6)	(+5.1)	(+6.4)	(–7.5)
B1AC2R						
0°	Exp.	0.041	–0.002	0.3513	0.4638	–0.1125
	Fluent	0.004	0.000	0.3039	0.4485	–0.1446
	(% diff.)	—	—	(–13.5)	(–3.3)	(–28.5)
10°	Exp.	–16.97	2.065	0.3746	0.5006	–0.1260
	Fluent	–17.34	2.070	0.3210	0.4849	–0.1639
	(% diff.)	(+2.1)	(+0.2)	(–14.3)	(–3.1)	(–30.1)
20°	Exp.	–43.31	5.465	0.3996	0.5324	–0.1328
	Fluent	–43.79	5.471	0.3470	0.5067	–0.1718
	(% diff.)	(+1.1)	(+0.1)	(–13.2)	(–4.8)	(–29.4)

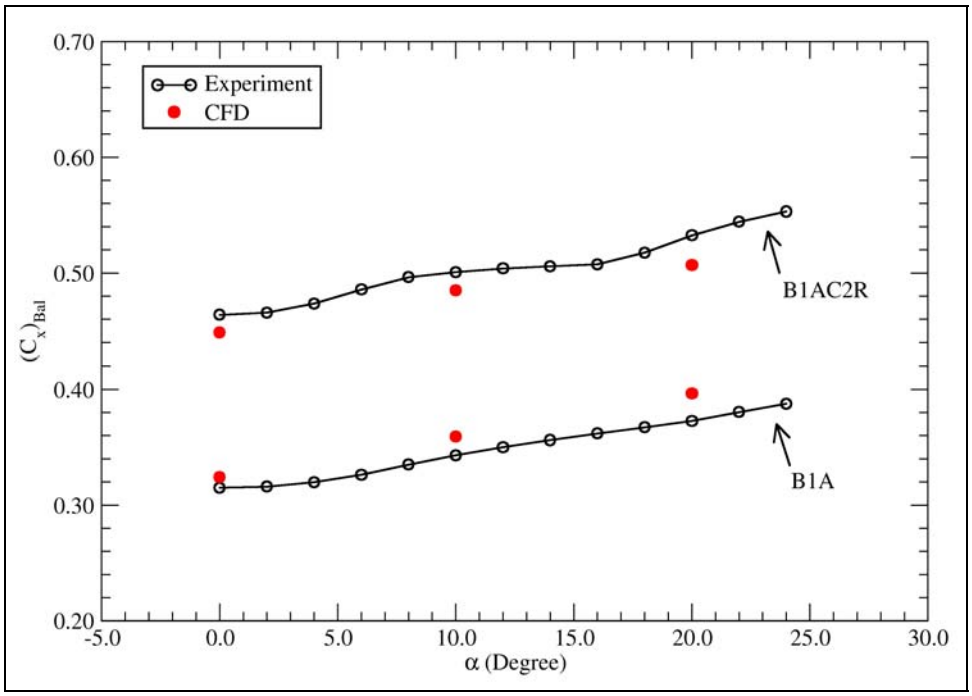

Figure 5. Total axial force coefficient vs. α for B1A and B1AC2R cases.

Again, the difference between the computed and measured forebody axial force is about 14%. From table 2, it can be seen that the discrepancy can be attributed to the measured base pressures used in the correction of the wind tunnel data, which are nominally 30% higher than the value computed in the CFD simulations. If the computed values of C_{pb} are used to determine C_x from the experimental $(C_x)_{Bal}$, the values are within 5% of those computed in the CFD simulations. This result is shown in figure 4, where the experimental forebody axial force curve has been shifted downward after adding the higher absolute value, CFD computed C_{pb} values to the total axial force values measured in the wind tunnel. We determined from DERA that the experimental base pressure was determined as the average pressure measured via two transducers located inside the hollow model on the balance. It is probable that the measurement in the planar fin case did not give an adequate representation of the average pressure over the base of the missile.

The computed C_{pb} is an average over the entire annular missile base, while the experimental C_{pb} is the average pressure measured in two locations inside the hollow model. A possible reason for the discrepancy between the computed and measured values in the planar fin case is that the pressure distribution is very nonuniform over the base. Figure 6 shows the pressure distributions (pressure coefficient, C_p, is plotted) on the base of the missile in body-alone and planar fin configurations for the three angles of attack investigated. The contours for the B1A case are, in general, more uniform than those for the corresponding B1AC2R case. The scale is the same in each plot, which tends to minimize the nonuniformity of the B1AC2R case at the lower values of α. Still, these plots indicate that the experimental base pressure measurement will be more dependent on the transducer location in the B1AC2R case. The nonuniformity in the pressure distribution grows with α in both configurations, but it is more significant in the B1AC2R case.

The likely cause for the nonuniformity is the wake behind the planar fins. Figure 7 shows that the flow in the wake region is significantly different in the presence of the fins, as should be expected. Figure 8 shows the pressure distribution on the surfaces of the missile and sting. The scale is too large to see details on the missile base, but differences in the pressure distribution for the two configurations are observed on the sting, especially at higher α.

A quantitative comparison of the results is shown in figure 9, which plots the pressure on the base of the missile as a function of azimuthal location (0° is the windward side, plots are symmetric about vertical plane). The profiles show the pressure at the junction of the sting and the missile base. At $\alpha = 0°$, the pressure is uniform in the body-alone case, as expected due to axisymmetry. The addition of the planar fins reduces the pressure behind the fins (0°, 90°, and 180°). At the higher angles of attack, the pressure distribution varies less for the body alone case, which is determined only by the wake of the missile. The pressure distribution in the

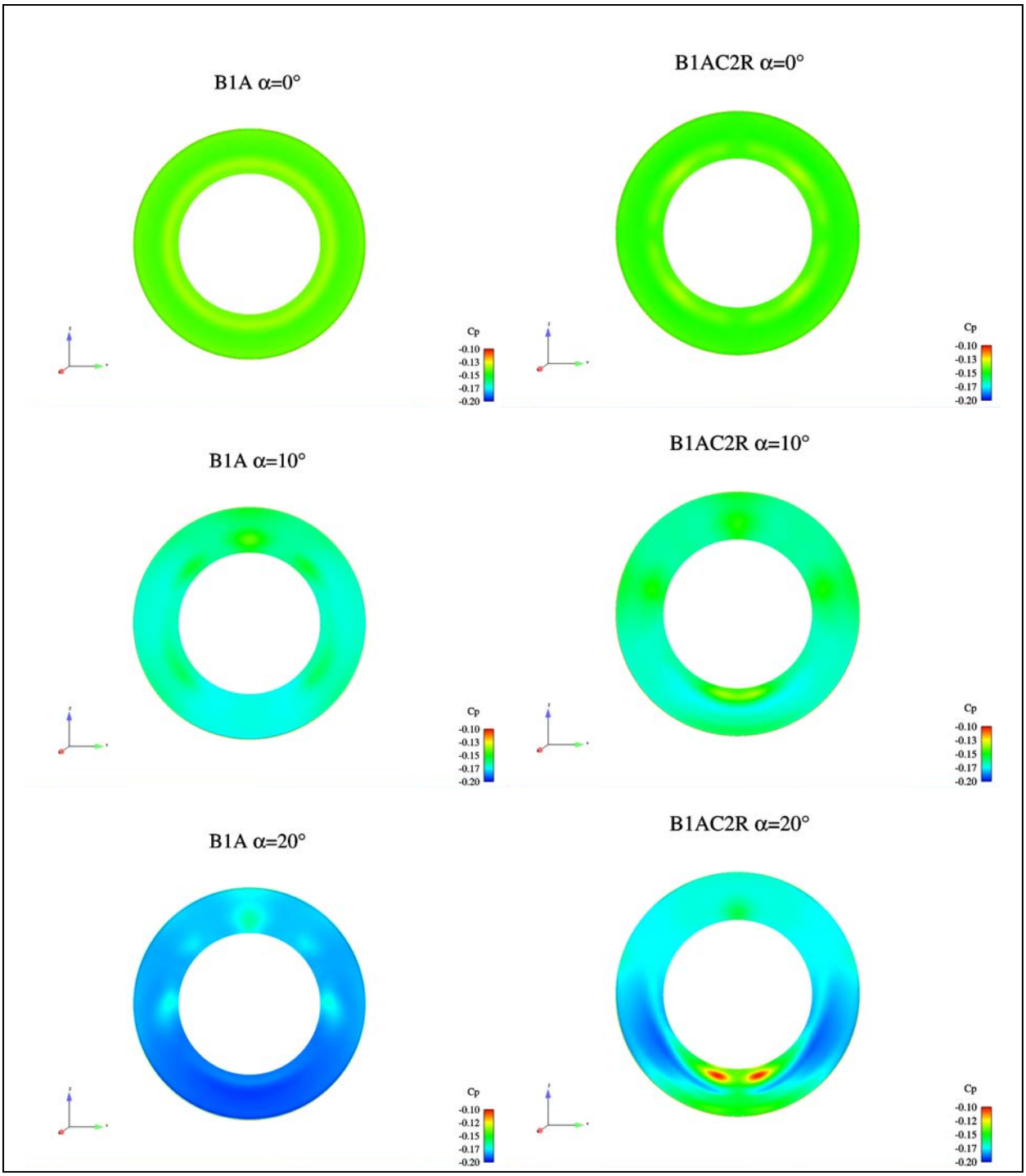

Figure 6. C_p contours on base of missile in B1A (left) and B1AC2R (right) configurations.

planar fin case is driven by a combination of the missile wake and the effect of the wake shedding from the planar fins. It can be seen from the plots in figure 9 that the azimuthal variation in pressure is higher for the planar fin case and this variation increases with angle of attack.

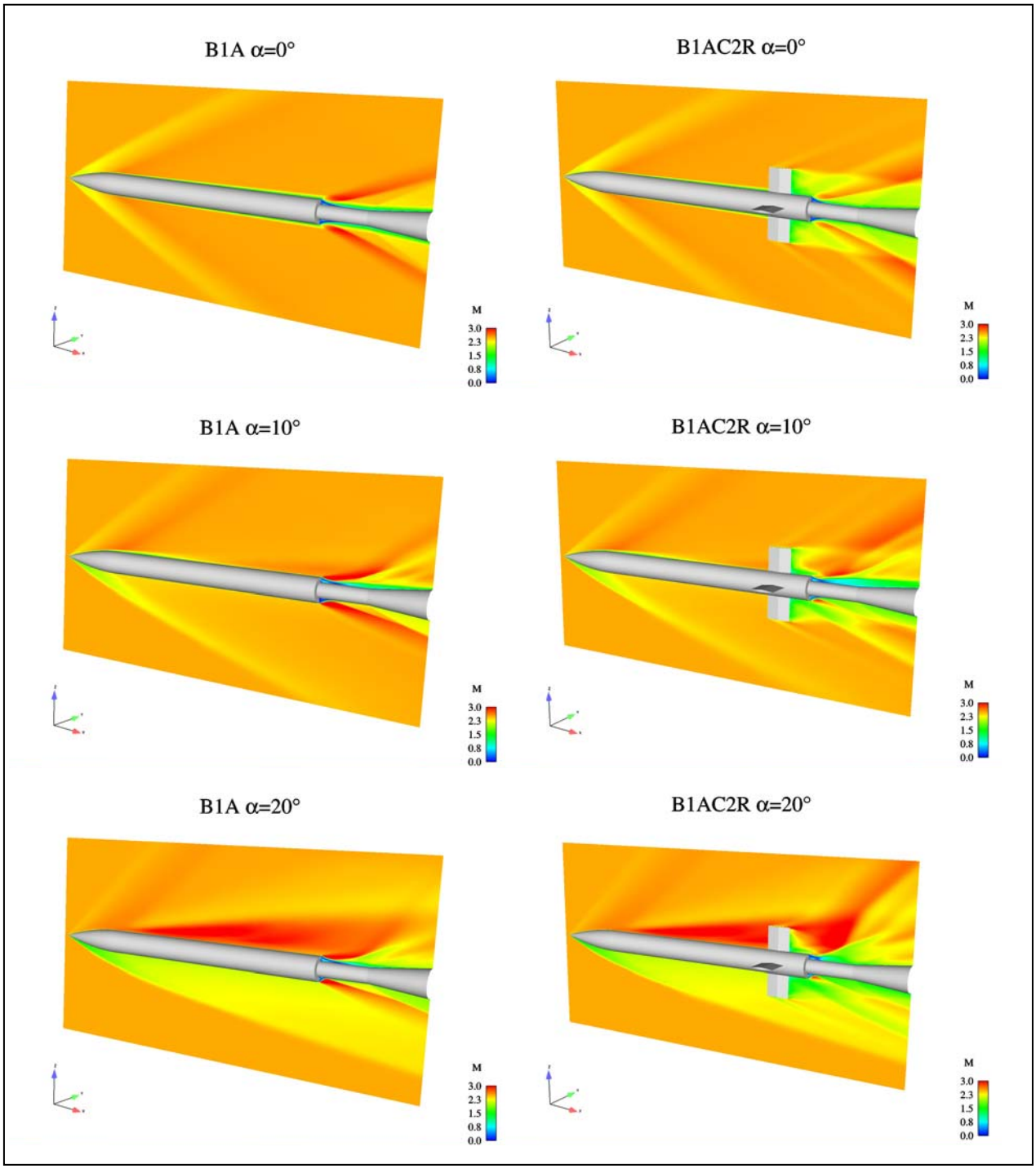

Figure 7. Mach number contours on symmetry plane in B1A (left) and B1AC2R (right) configurations.

Although it cannot be definitively said that the experimental base pressure measurement is inaccurate, the present results give a strong indication of such. It is noted again that the computed and measured total axial force are in excellent agreement in both configurations. It must be stressed that the quality of the DERA wind tunnel data for the three configurations investigated in DeSpirito et al. (*1–3*) was excellent. The discrepancy in the forebody axial force

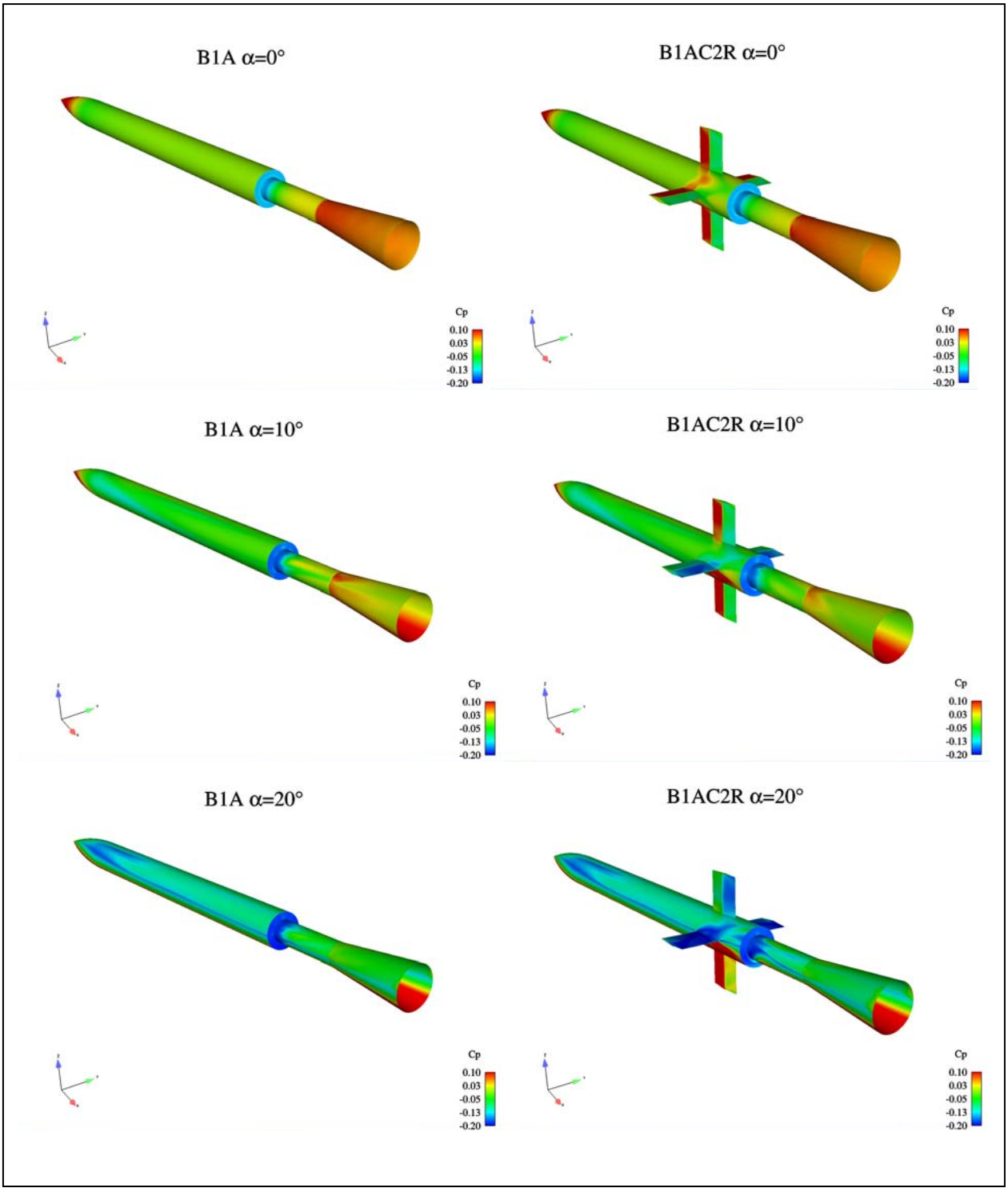

Figure 8. C_p contours on missile and sting surfaces in B1A (left) and B1AC2R (right) configurations.

is only stressed as an explanation for differences in the CFD computed values for this force. It was puzzling since all other forces were predicted very well, even the forebody axial force in the other missile configurations.

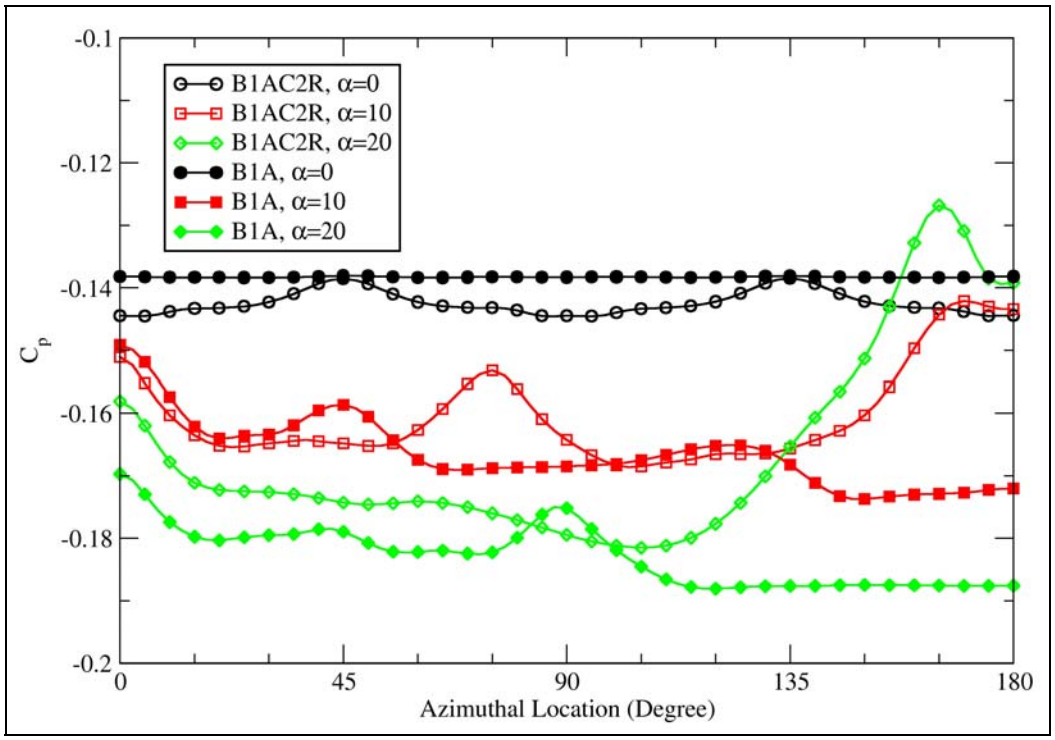

Figure 9. C_p profiles on base of missile.

4. Summary

CFD was used to compute the aerodynamic coefficients of two missile configurations in the presence of a wind tunnel sting. The results were compared to the results of a previous investigation in which the computed forebody axial force did not compare well with the experimental wind tunnel data. The current investigation showed that the computed results are accurate, predicting the total axial force to within 5% of the experimental values. However, the investigation also indicated that experimental base pressure measurement did not give an accurate representation of the average base pressure when the model had planar fins. The base pressure measurement was apparently adequate for the body alone case and for the model with grid fins. In the grid fin case, wake behind the fins is more diffuse, likely reducing the effect on the base of the missile.

5. References

1. DeSpirito, J.; Edge, H. L.; Weinacht, P.; Sahu, J.; Dinavahi, S. *CFD Analysis of Grid Fins for Maneuvering Missiles*; AIAA-2000-0391; American Institute of Aeronautics and Astronautics, January 2000.

2. DeSpirito, J.; Edge, H. L.; Weinacht, P.; Sahu, J.; Dinavahi, S. *Computational Fluid Dynamic (CFD) Analysis of a Generic Missile with Grid Fins*; ARL-TR-2318; U.S. Army Research Laboratory: Aberdeen Proving Ground, MD, September 2000.

3. DeSpirito, J.; Edge, H. L.; Weinacht, P.; Sahu, J.; Dinavahi, S. Computational Fluid Dynamic Analysis of a Generic Missile with Grid Fins. *J. Spacecraft and Rockets* **2001**, *38* (5), 711–718.

4. Spalart, P. R.; Allmaras, S. R. A One-Equation Turbulence Model for Aerodynamic Flows, AIAA-92-0439, American Institute of Aeronautics and Astronautics, January 1992.

5. Fluent, Inc. *Fluent 5.0 Users Guide*, Vol. 2; Fluent, Inc.: Lebanon, NH, 1998.

NO. OF
COPIES ORGANIZATION

1 (PDF ONLY) DEFENSE TECHNICAL INFORMATION CTR
DTIC OCA
8725 JOHN J KINGMAN RD
STE 0944
FORT BELVOIR VA 22060-6218

1 US ARMY RSRCH DEV & ENGRG CMD
SYSTEMS OF SYSTEMS INTEGRATION
AMSRD SS T
6000 6TH ST STE 100
FORT BELVOIR VA 22060-5608

1 INST FOR ADVNCD TCHNLGY
THE UNIV OF TEXAS
AT AUSTIN
3925 W BRAKER LN
AUSTIN TX 78759-5316

1 DIRECTOR
US ARMY RESEARCH LAB
IMNE ALC IMS
2800 POWDER MILL RD
ADELPHI MD 20783-1197

3 DIRECTOR
US ARMY RESEARCH LAB
AMSRD ARL CI OK TL
2800 POWDER MILL RD
ADELPHI MD 20783-1197

3 DIRECTOR
US ARMY RESEARCH LAB
AMSRD ARL CS IS T
2800 POWDER MILL RD
ADELPHI MD 20783-1197

ABERDEEN PROVING GROUND

1 DIR USARL
AMSRD ARL CI OK TP (BLDG 4600)

NO. OF
COPIES ORGANIZATION

1 AFRL/MNAV
G ABATE
101 W EGLIN BLVD STE 332
EGLIN AIR FORCE BASE FL 32542

1 AEROPREDICTION INC
F MOORE
9449 GROVER DR STE 201
KING GEORGE VA 22485

1 UNIV OF TEXAS AT ARLINGTON
MECHANICAL AND AEROSPACE
ENGR DEPT
J C DUTTON
BOX 19018
500 W FIRST ST
ARLINGTON TX 76019-0018

3 COMMANDER USAAMCOM
AMSAM RD SS AT
R KRETZSCHMAR
L AUMAN
E VAUGHN
REDSTONE ARSENAL AL 35898-5252

ABERDEEN PROVING GROUND

16 DIR USARL
AMSRD ARL CI HC
R NOAK
AMSRD ARL WM
J SMITH
AMSRD ARL WM B
T ROSENBERGER
AMSRD ARL WM BA
J DESPIRITO (3 CPS)
B GUIDOS
K HEAVEY
P PLOSTINS
J SAHU
S SILTON
P WEINACHT
AMSRD ARL WM BD
B FORCH
M LEADORE
AMSRD ARL WM BF
H EDGE
S WILKERSON

NO. OF
COPIES ORGANIZATION

1 DSTL BEDFORD
T BIRCH
BLDG 115 RM 125
BEDFORD TECHNOLOGY PARK
BEDFORD
MK44 2FQ
UK

1 DSTL FORT HALSTEAD
J EDWARDS
SEVENOAKS KENT
TN 14 7BP
UK

2 DEFENCE RSCH AND
DEV CANADA-VALCARTIER
F LESAGE
E FOURNIER
2459 PIE XI BLVD N
VAL-BELAIR (QC) G3J1X5
CANADA

1 DEFENCE SCIENCE AND
TECHNOLOGY ORGANIZATION
V BASKARAN
BLDG 11 RM 119
506 LORIMER ST
FISHERMANS BEND
VICTORIA 3207
AUSTRALIA